SPC

Advanced Journal of Chemistry-Section A

Journal homepage: www.ajchem-a.com

Original Research Article

Synthesis and Characterization of a Nanomagnetic Adsorbent Modified with Thiol for Magnetic and its Adsorption Behavior for Effective Elimination of Heavy Metal Ions

Parisa Nejati, Somayyeh Rostamzadeh Mansour*, Nastaran Sohrabi-Gilani

Department of Chemistry, Ardabil Branch, Islamic Azad University, Ardabil, Iran

ARTICLE INFO

Article history

Submitted: 02 October 2021
Revised: 29 October 2021
Accepted: 18 November 2021
Available online: 20 November 2021
Manuscript ID: AJCA-2110-1283
Checked for Plagiarism: Yes

DOI: 10.22034/AJCA.2021.308695.1283

KEYWORDS

Nanomagnetic adsorbent
Thiourea formaldehyde polymer
Adsorption behavior
Removal of heavy metal ions

ABSTRACT

The main purpose of the current research was the synthesis of a novel nanomagnetic adsorbent modified with Thiol containing groups and investigating its adsorption behavior for effective elimination of heavy metal ions from environmental waters. To this end, first, the co-precipitation method was utilized to prepare Thiol-modified magnetite nanoparticles (NPs). Then, the surface of magnetic NPs was modified with Thiourea formaldehyde polymeric material, followed by purification and identification of the synthesized products. Finally, the efficiency and performance of the synthesized nanoparticles for heavy metal ions removal were investigated in the aqueous solution. The synthesis mechanism of modified nanomagnetic adsorbents were investigated and identified through various analyses including (FT-IR), (XRD), (SEM) and (VSM). The results indicated that modified nanomagnetic adsorbents were able to remove and extract the chromium (II) and cobalt (II) from aqueous solutions. Further, Langmuir and Freundlich adsorption isotherms were studied and the results showed that adsorption data of both analytes were fitted well with Langmuir isotherm. Thus, the single-layer adsorption mechanism and the homogeneous adsorbent surface can be considered.

GRAPHICAL ABSTRACT

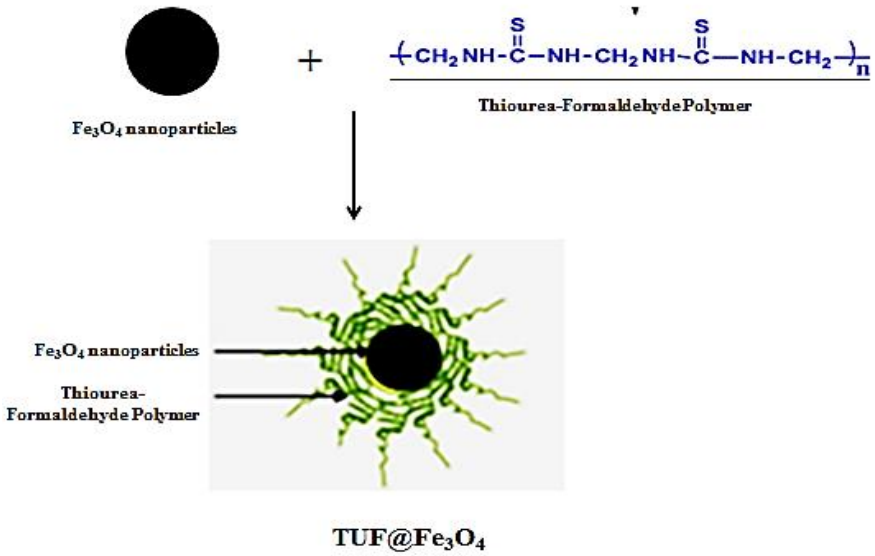

* Corresponding author: Rostamzadeh Mansour, S.
✉ E-mail: somayyehrostamzade@gmail.com

Introduction

Water pollution with heavy metals, due to its chemical stability and the ability to accumulate in the living bodies, is a global health problem. High levels of these metals increase mortality, morphological disorders, growth retardation and genetic effects in humans [1-4]. Heavy metals can be originated from two classes of sources: Natural sources involving erosion processes, weathering of rocks and minerals, and volcanic activity and man-made origins such as mining, fuel combustion, traffic, and agricultural activities. These activities can degrade water quality for drinking, agricultural and industrial uses. The presence of heavy metals in the drinking water for infants and young children can cause dementia and learning disabilities, memory impairment, damage to the nervous system, and movement disorders such as seizures or hyperactivity. In fact, it can be said that the main source for toxic metals entering to water is municipal wastewater and industrial effluents. The rise in the population of cities and the industrial progress have led to widespread contamination of drinking water, especially heavy metals [5-7]. Various water treatment approaches, including mechanical, biological, physical, and chemical, have been developed. Among them, adsorption has exhibited promising potential for removal of metal ions residual from previous purification processes. Inorganic sorbents have shown high resistance to heat, radiation, and organic solvents in addition to excellent selectivity and regeneration. Despite the versatility of magnetic nanomaterials, some weak points have remained unresolved among which, difficult synthesis, costly reagents, poor stability, and reusability can be mentioned. Coating magnetic NPs with silica shells with high chemical stability, the possibility of surface modification, and biocompatibility can prevent the oxidation or dissolution of these NPs at low pH values [8]. Accordingly, the surface of inorganic adsorbents can be modified by diverse complex and chelate groups capable of forming stable complexes with metal ions.

Actually, the chemical adsorption is the covalent bond creation between the adsorbent and the absorbed material. Nowadays, extensive research has been done to increase the efficiency of adsorbents around the world, and in recent years the nanosorbents have attracted special attention for the removal of heavy metals [9-13]. Elwakeel *et al*. used a functionalized magnetic adsorbent with Mercapto group to extract the solid phase of inert metals and applied flame atomic absorption spectrometry (FAAS) to measure them. The results showed that the recovery percentage of these metals (Au, Ir, Pt, Pd, Rh, Ru) was about 90% [14]. Al-Rashdi *et al*. used Fe_3O_4 magnetic nanoparticles coated with Decanoic acid as an adsorbent for solid phase extraction. They investigated the determination of partial measurements of cadmium, cobalt, chromium, nickel, lead and zinc from natural and ambient water samples by using flow injection (Injection flow) of (FAAS) [15]. Polymeric monoliths based on acrylonitrile-divinyl benzene were synthesized successfully by high internal phase emulsion (HIPE) polymerization by Wasif Shaikh *et al.* [16]. Highly porous polyHIPEs were prepared by variation in oil to water ratio as well as type and concentration of porogens. The porogens evaluated were toluene, chlorobenzene, heptane and chloroform. The effect of oil to water ratio and porogen type and concentrations on morphology and surface area of polyHIPEs were investigated. The polyHIPEs were modified to amidoxime functionality by treating base catalyzed reaction with hydroxylamine hydrochloride in presence of base. The treated and modified polymeric monoliths were characterized by FT-IR, SEM and surface area analysis. The modified porous polyHIPEs were tested for adsorption of Cr(VI) metal ions at various pH [16]. Ranjhan Junejo et al. studied the synthesis of the p-

piperdinomethyl calix arene attached silica (PAS) resin and to investigate their metal ions removal efficiency from water [17]. In batch adsorption experiment, PAS resin shows good adsorption efficacy for the Cu^{2+} and Pb^{2+} metal ions. Furthermore, thermodynamics and kinetic study revealed that the adsorption process spontaneity and endothermic followed the pseudo 2nd order kinetic equation with good regression coefficient[17]. Dehno Khalaji et al. studied the as-prepared α-Fe_2O_3 nanoparticles used as photocatalyst for degradation and removal of methyl orange (MO) dye under visible light irradiation from aqueous solution [18]. The influence of various parameters such as contact time and dosage of catalyst were examined and discussed. The study revealed that the degradation of MO reached 95% (Fe-1), 88% (Fe-2) and 62% (Fe-3) within 120 min by increasing of catalyst dosage from 0.02 g to 0.06 g. Degradation rates of MO by Fe-1, Fe-2 and Fe-3 were 0.0249, 0.0177 and 0.0081 min-1, respectively, indicating that the degradation depended on the crystalline size and morphology of the α-Fe_2O_3 magnetic nanoparticles [18]. Magnetically functionalized materials (adsorbents) can be quickly removed from the sorption through facile approaches. Moreover, their modification can be easily achieved using any required functional groups. In this study, magnetite nanoparticles modified with sulfur groups were prepared through a co-precipitation approach. The synthesized products were purified and identified. Finally, the efficiency and performance of the synthesized nanoparticles for removing heavy metal ions from aqueous solutions has been investigated. As an analytical method, magnetic solid-phase extraction (MSPE) employs magnetic adsorbents for the separation and preconcentration of diverse organic and inorganic analytes from solutions. A typical MSPE process involves the use of magnetic adsorbents which will be contacted with the target analyte for a predetermined time followed by analyte separation [19, 20].

Experimental

Synthesis of magnetite nanoparticles

The $FeCl_2$.$4H_2O$ (1.075 gram) and $FeCl_3$. $6H_2O$, (2.92 gram) were weighed and dissolved at 80 mL water in a three necked flask, and placed on the Heater Stirrer. After denitrogenation of the solution, it underwent 80 °C. After 15 minutes, 25 mL of ammonia was added to the solution dropwise to form a black precipitate. The contents of the three necked flasks were entered to a beaker and the product was separated from the solution easily and magnetically before being separated. Then, the product was washed by ethanol and distilled water for several times, and dried at ambient temperature (Figure 1).

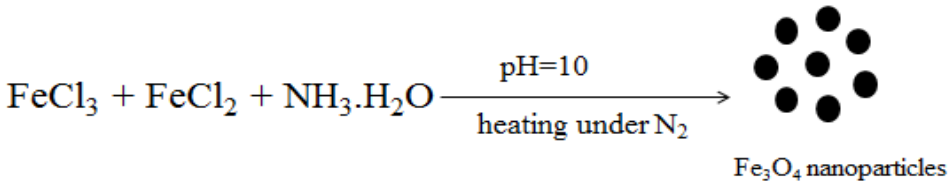

Figure 1. Mechanism of the synthesis of magnetite NPs

Synthesis of thiourea-formaldehyde

After dissolving 1.52 g thiourea in 10 mL methanol, 1.5 mL formaldehyde solution was added to them, the pH of a solution was adjusted to 3. The mixture was refluxed at 90 °C until to form a white or colorless viscosity product. Then, the obtained product was washed by acetone, methanol and deionized water (Figure 2).

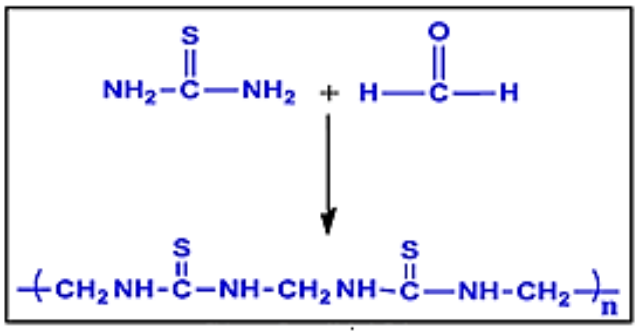

Figure 2. The mechanism of thiourea-formaldehyde synthesis

Synthesis of magnetite nanoparticles coated with thiourea-formaldehyde polymer

To prepare the desired nanosorbent, 1 gr of magnetite obtained and 0.1 gram of urea-formaldehyde obtained were dissolved in deionized water (50 mL), followed by 24 hours of stirring and then rinsing with deionized water (Figure 3).

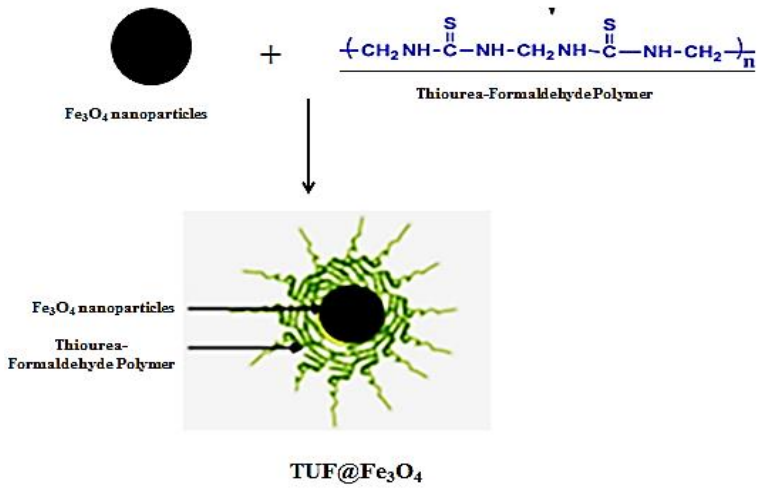

Figure 3. Nanosorbent synthesis mechanism

Results and Discussion

Magnetite NPs were prepared using iron (II) and (III) salts (with a stoichiometric ratio of 1: 2) were applied by using the co-precipitation method. This reaction is sensitive to air oxygen and moisture. In the second step, the obtained magnetite nanoparticles were coated with polymer (thiourea-formaldehyde). Polymer-coated magnetite nanoparticles were used as nanosorbents to remove the heavy metals.

FT-IR patterns of magnetite nanoparticles

Figure 4 presents the FT-IR spectrum of the prepared magnetite nanoparticles. Two peaks related to the Fe-O bonding are seen in magnetite particles at 568 and 435 cm^{-1}. Three peaks observed at 3415, 11620, and 800 cm^{-1} are related to the off-plane stretching and flexural vibrations of the surface hydroxyl groups, respectively.

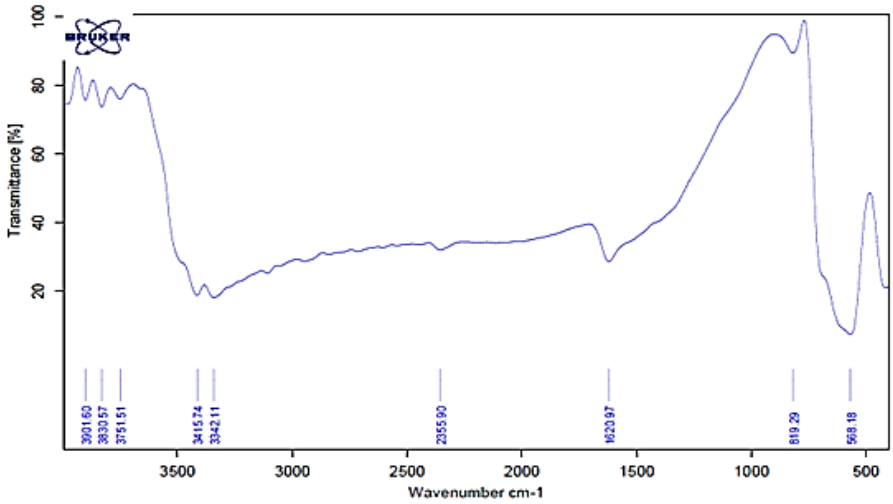

Figure 4. FT-IR spectrum of magnetite nanoparticles

FT-IR spectrum for Nano magnetite coated with thiourea- formaldehyde polymer

Figure 5 depicts the FT-IR spectrum of magnetite nanoparticles coated with thiourea-formaldehyde polymer. The TUF polymer spectrum has a strong adsorption band at 3308 cm^{-1}, indicating this strong peak is related to NH composition. Two strong adsorption bands at 1617 and 1545 cm^{-1} can be attributed to the C=S amide group. The observed bands at 1005 and 1072 cm^{-1} can be assigned to C-N vibration, the observed peaks at 1330 and 1438 cm^{-1} are related to CH_2 flexural vibration and the observed peak at 2954 cm^{-1} is related to CH_2 stretching vibrations. In addition to the observed peaks for the polymer, the Fe-O peaks are observed at 1442 and 523 cm^{-1}, indicating that the polymer covers the surface of magnetite NPs.

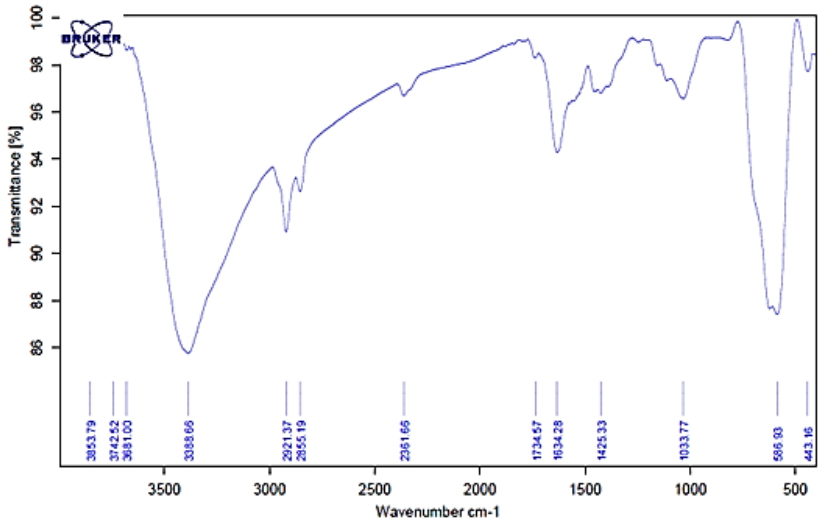

Figure 5. FT-IR spectrum of magnetic NPs coated with thiourea formaldehyde polymer

XRD pattern of magnetite and nanomagnet nanoparticles coated with polymer thiourea formaldehyde

Figures 6a and 6b present the X-ray diffraction patterns of magnetite NPs and those coated with thiourea-formaldehyde, respectively. All

observed peaks at these patterns correspond to the reported data from the standard XRD model (2267 86 JCPDS card No) and confirm the nanoparticle crystallinity. The XRD pattern of Fe_3O_4 nanoparticles is shown in Figure 6a, showing that Fe_3O_4 nanoparticles with the cubic spinel structure of peaks at (440), (511), (422), (400), (311), (220). For all samples, the absence of peaks (110) (2θ = 21.220) and (104) (2θ = 33.150) indicates that both phases of guillotine (α FeOOH) and hematite (α Fe_2O_3) are not formed in the samples. Average crystallite sizes were then solved using Scherrer equations as shown in Equation (1), in which K shows the shape factor (K = 0.9), while λ denotes the X-ray wavelength (λ = 0.154 nm). β represents the width of the highest half-height peak (FWHM) and θ stands for the diffraction angle. The average size of Fe_3O_4 nanoparticles was 30.8 nm using the highest peak width (311) and thiourea formaldehyde was 40.76 nm. Figure 6b shows that the observed peaks for the spinel phase are wider, which can be attributed to the polymer coating on the nanoparticle surface. The XRD data of magnetite NPs and nanomagnetite coated with thiourea-formaldehyde polymer are given in Table 1.

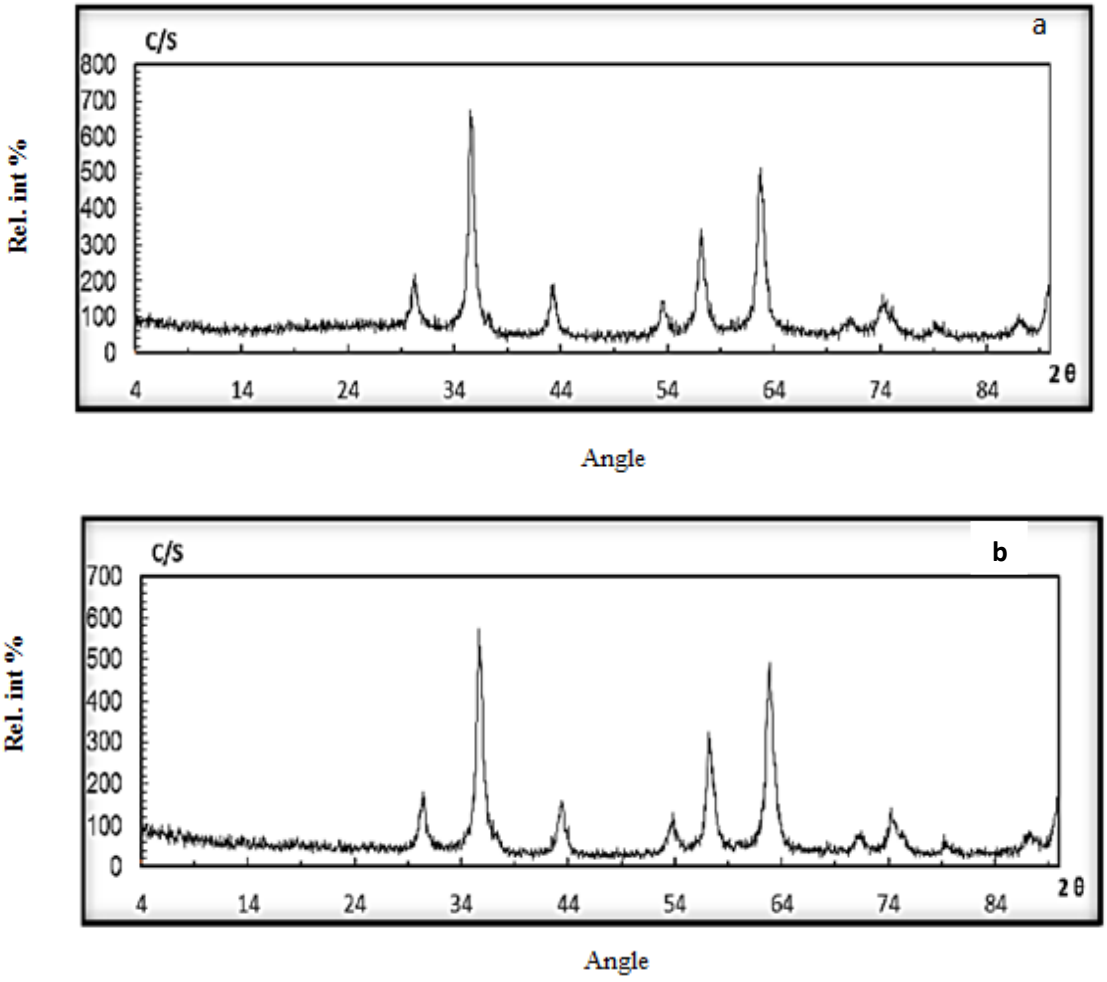

Figure 6. XRD results of (a) magnetite NPs and (b) thiourea-formaldehyde-coated magnetite NPs

Table 1. XRD data of (a) magnetite nanoparticles and (b) nanomagnetite coated with thiourea-formaldehyde

(a)

Angle	d-value	Rel. int.	Angle	d-value	Rel. int.
2 Teta	Angstrom	%	2 Teta	Angstrom	%
18.680	4.746	1.6	74.300	1.276	11.8
30.225	2.954	23.4	79.190	1.209	4.4
35.515	2.526	100.0	87.035	1.119	5.5
37.255	2.412	5.4			
43.155	2.095	21.4			
53.555	1.710	14.1			
57.165	1.610	45.9			
62.690	1.481	70.4			
63.000	1.474	57.2			
71.105	1.325	4.6			

(b)

Angle	d-value	Rel. int.	Angle	d-value	Rel. int.
2 Teta	Angstrom	%	2 Teta	Angstrom	%
7.580	11.653	2.8	68.370	1.371	2.1
18.770	4.724	2.3	71.285	1.322	6.4
21.670	4.098	2.0	74.220	1.277	14.1
24.845	3.581	1.1	79.390	1.206	4.0
30.475	2.931	19.2	87.265	1.116	5.7
35.680	2.514	100.0			
43.515	2.078	21.2			
53.815	1.702	14.1			
57.195	1.609	45.8			
62.865	1.477	85.5			

θ : Separation angle; $Fwhm$: Half the height at the highest peak in radians; β : The width of the; tallest peak at half height; k : shape constant (0.9); λ : X-ray wavelength (0.154 nm);

d : Average value of particle size

$$d = \frac{k.\lambda}{\beta.\cos\theta} \quad (1)$$

SEM images of synthesized samples

SEM images of magnetite nanoparticles and magnetite nanoparticles coated with thiourea-formaldehyde polymer are shown in Figures 7a and 7b, respectively. All SEM images signify homogeneous distribution of spherical nanoparticles.

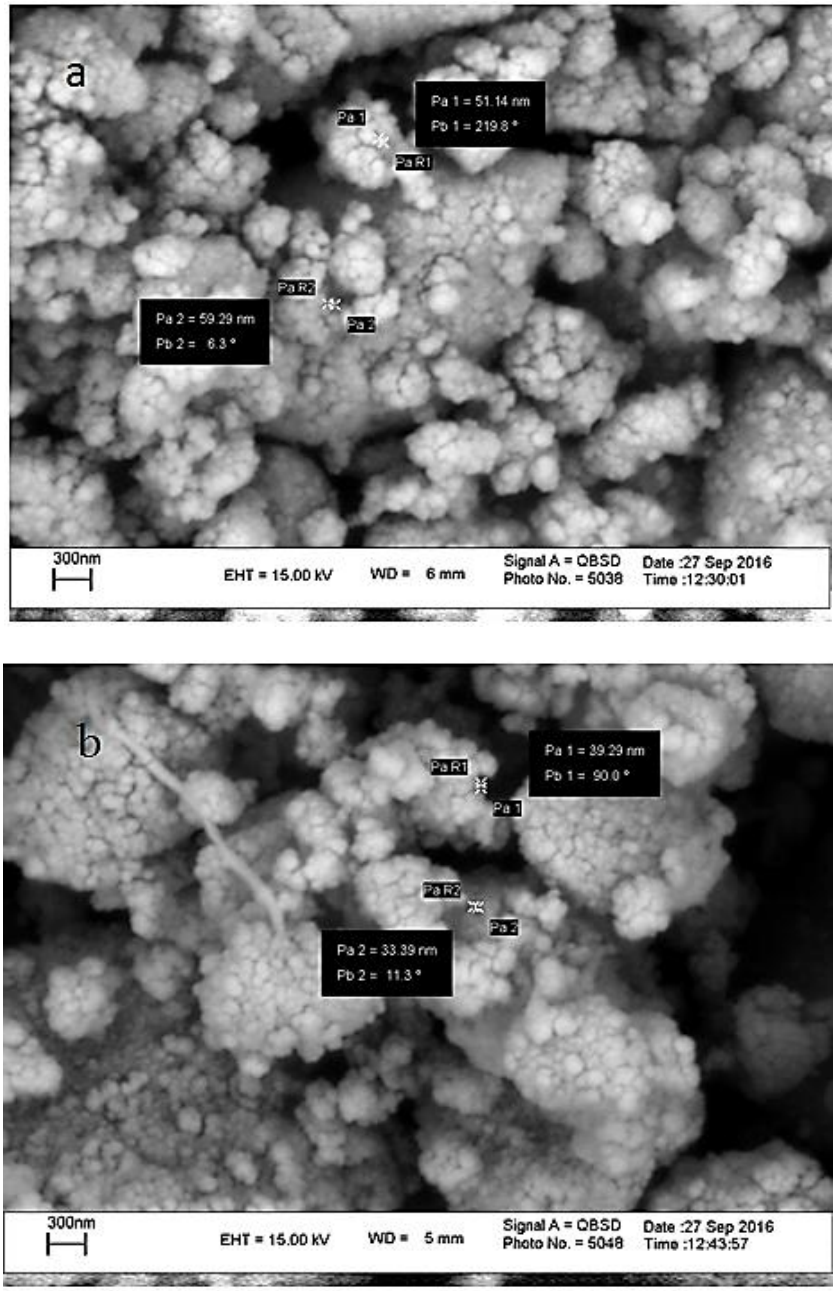

Figure 7. SEM image of (a) Magnetite nanoparticles (b) Nanomagnetite coated with thiourea-formaldehyde polymer

Investigation of magnetic properties of magnetite nanoparticles and nanomagnet nanoparticles coated with polymers

Figures 8a, b and Table 2 show the magnetic field-dependent magnetization M (H) of Fe_3O_4 and Fe_3O_4@TUF NPs at room temperature using a vibrating sample magnetron in the KOe 15 field. The superparamagnetic behavior of Fe_3O_4 can be verified by the absence of a residual loop in its corresponding magnetism diagram. The superparamagnetic features of this compound can be also confirmed regarding its saturation magnetization (60 emu/g at a temperature of 300 k). VSM diagram of polymer-coated magnetite NPs also indicated their superparamagnetic properties due to the

absence of a waste ring. However, a decline can be observed in the saturation magnetization of this compound (56 emu/g), suggesting a decrease in the magnetic properties as a result of coating with a polymer, which is reduced compared with the original magnetite due to the establishment of the coating groups around the magnetite substrate.

Table 2. Magnetic parameters of Fe_3O_4 and Fe_3O_4@TUF nanoparticles

Samples	Ms (emu/g)	Hc (Oe)
Fe_3O_4	60 emu/g	0
Fe_3O_4@TUF	56 emu/g	0

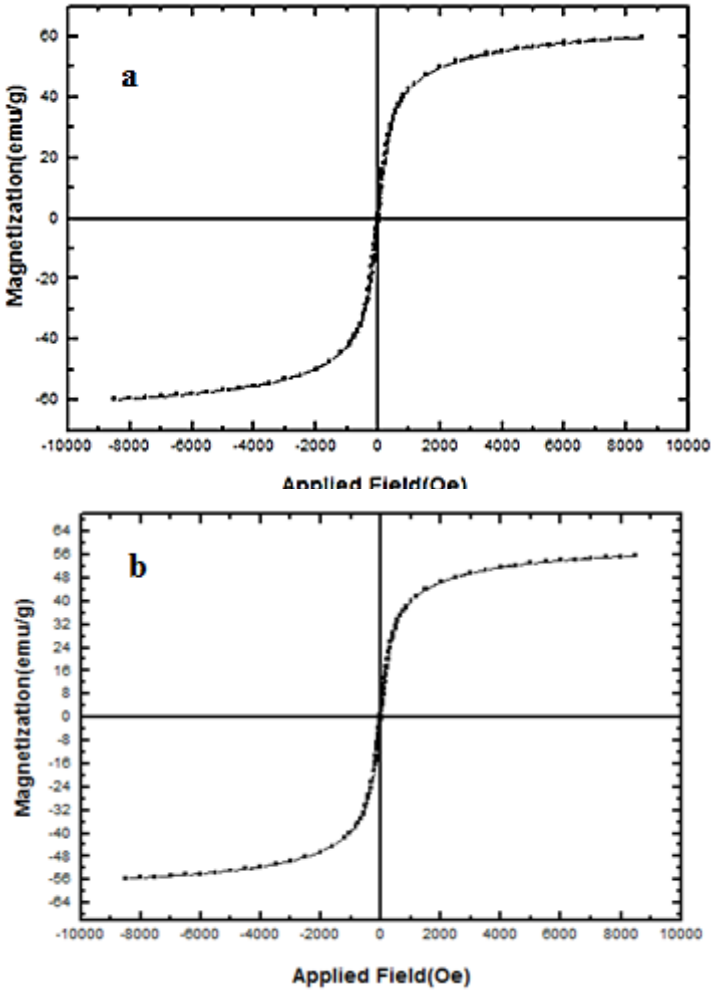

Figure 8. The Magnetization vs. magnetic field for (a) Fe_3O_4 NPs and (b) Fe_3O_4@TUF NPs

Evaluation of the adsorbent performance

Adsorption ability and efficiency of the prepared adsorbent in removal of heavy metal ions were evaluated under batch mode. Adsorption behavior was explored by adding of 10 mg of the adsorbent into 20 mL solution containing one of the target heavy metal ions (2 mg L^{-1}) at pH=7. pH was set using diluted nitric acid (0.1 M) and sodium hydroxide (0.1 M). After stirring the solution (10 min at 200 rpm), a strong magnet was placed at the bottom of the beaker for 2 min. The supernatants can then be easily decanted. The heavy metal concentration

of the decanted solution was evaluated by FAAS. The removal percentage (%R) was assessed using the following equation:

$$\% R = \frac{(C0 - C)}{C0} \times 100 \quad (2)$$

in which C_0 and C show the analyte concentrations in the initial sample and final solutions, respectively.

Among the various studied heavy metal ions (Cd(II), Ni(II), Co(II), Cu(II), Fe(III), Zn(II), Cr(III), Pb(II), and Ag(I)), the adsorbent showed high adsorption tendency to Co(II) and Cr(III) as they were only quantitatively adsorbed with the adsorbent (%R=100).

Adsorption studies

As mentioned earlier, the adsorbent showed high tendency to Cr(III) and Co(II) and completely removed them from aqueous solution.

Effects of stirring time, pH, and eluting solvent concentration were studied and optimized. The influence of pH on Cr(III) and Co(II) adsorption was assessed in the pH range of 2-8. To this end, 10.0 mg adsorbent was mixed in 100 mL solution containing 10 µg of the mentioned ions in the 250 mL beaker and each time; the pH was adjusted to desired pH (in the range of 2 to 8) with diluted HCl and NaOH solutions. The solution was stirred for 10 min at 200 rpm. Then, a strong magnet was placed under the beaker. Within 2 minutes, the mixture became clear and a magnetic adsorbent was settled at the bottom of the beaker. The clear solution was easily decanted and the concentration of Cr(III) and Co(II) in this solution was assayed using FAAS and %R of each metal ion was evaluated. The plot of %R versus pH is shown in Figure 9. It is obvious that in pH=7, both metal ions are removed completely from the aqueous solution.

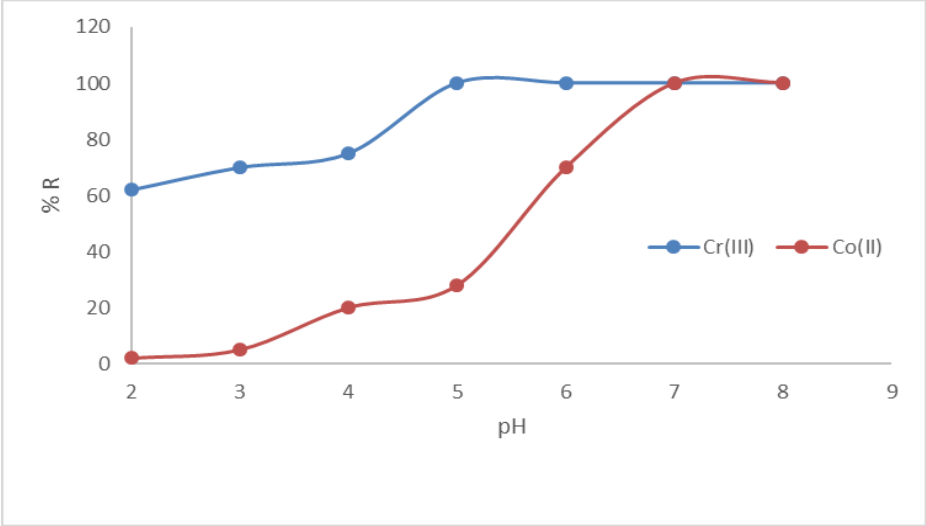

Figure 9. Influence of pH on the removal percentage of Cr(III) and Co(II)

To investigate the role of stirring time in the Cr(III) and Co(II) adsorption, the above mentioned procedure was performed in pH=7 but stirring time was changed in the range of 2 - 20 min. The results revealed that %R of two metal ions reached 100% in 10 min that is indicative of a very fast adsorption process.

In order to study the effect of desorbing solvent concentration, 5 mL of HNO_3 solution, with concentration in the range of 0.1-3 M, was added to the adsorbent for eluting the adsorbed metal

ions from the adsorbent surface followed by 5 minutes of stirring. Subsequently, the adsorbent was magnetically separated and the concentration of each metal ion was quantified in elution solution through the FAAS method. It was revealed that 5 mL of 1 M HNO_3 solution was able to complete recovery of two metal ions. Therefore, this magnetic adsorbent can be used effectively in the magnetic solid phase extraction of these metal ions.

Adsorption isotherms and adsorbent capacities

The adsorption behavior was modeled to determine the adsorption capacity by evaluating two adsorption isotherms (Langmuir and Freundlich). For this purpose, 10 mg adsorbent was added to 20 mL solutions containing different primary concentrations of Cr(III) or Co(II) in the range of 20-150 mg L^{-1} adjusted to pH=7 at 25 °C. One hour of stirring was carried out to ensure the realization of equilibrium. Then, the magnetic adsorbent was separated from the solution and metal ion concentration in the solution was measured using FAAS.

The Langmuir isotherm model relies on the homogenous adsorbent surface possessing a finite number of identical adsorption sites [21] with monolayer adsorption behavior as described:

$$q_e = q_{max} \frac{K_L C_e}{1+K_L C_e} \quad (3)$$

In the above equation, C_e (mg L^{-1}) shows the equilibrium concentration of the metal ion while q_e (mg g^{-1}) denotes the equilibrium adsorption capacity. K_L also stands for Langmuir constant (L mg^{-1}). The larger K_L is corresponding to more intense adsorption, and q_{max} (mg g^{-1}) represents the maximal adsorption capacity corresponding to a full monolayer coverage.

The linear form of Langmuir model is more suitable for calculating the isotherm parameters and is given by:

$$\frac{C_e}{q_e} = \frac{1}{q_{max} K_L} + \frac{C_e}{q_{max}} \quad (4)$$

The Freundlich isotherm refers to an empirical equation on the basis of highly heterogeneous surface adsorption resulted in multilayer adsorption. This isotherm can be described by a linearized equation:

$$\text{Ln } q_e = \ln K_F + \frac{1}{n} \ln C_e \quad (5)$$

In which, K_F denotes Freundlich constants indicative of adsorption capacity and n represents adsorption intensity, which varies with the heterogeneity of the adsorbent. The values of $1/n > 2$ and $0.1 < 1/n < 0.5$ are indicative of unfavorable and favorable adsorptions, respectively.

The plots of Langmuir and Freundlich models for Cr(III) and Co(II) adsorption onto the prepared adsorbent, and the corresponding fitting parameters are listed in Figures 10a, b, 11a, b and Table 3.

It is evident from the obtained results that the Langmuir equation fitted well the experimental data of both metal ion adsorption with a higher correlation coefficient compared to Freundlich equation. Accordingly, the single-layer adsorption mechanism by a homogeneous adsorbent can be concluded [22].

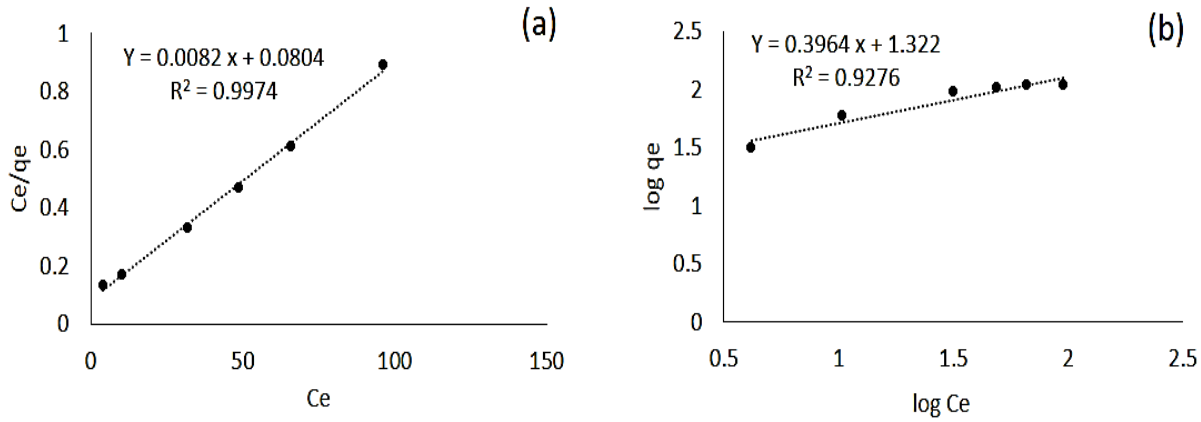

Figure 10. Adsorption isotherms of Cr(III): (a) Langmuir and (b) Freundlich models

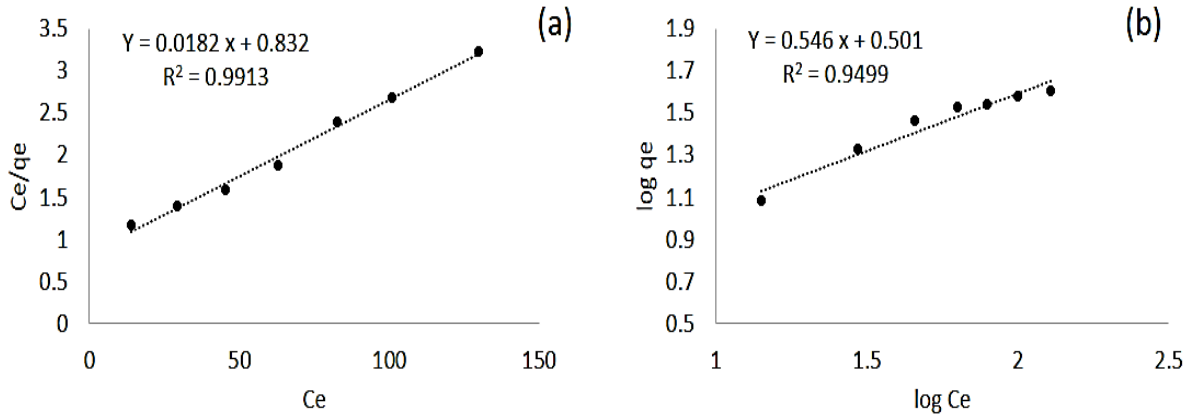

Figure 11. Adsorption isotherms of Co(II): (a) Langmuir and (b) Freundlich models

Table 3. Parameters calculated from the fitting results for Lamgmuir model

Analyte	q_{max} (mg g^{-1})	KL (L mg^{-1})	R^2
Cr^{3+}	121.95	0.101	0.9974
Co^{2+}	54.94	0.021	0.9913

Conclusion

In this study, magnetic nanosorbents consisting of magnetite nanoparticles modified with thiourea formaldehyde polymer were prepared by co-precipitation method and identified by FT-IR, XRD, SEM, and VSM techniques. Magnetic measurements were demonstrated for nanosorbent. Surface modification of the magnetic NPs with thiourea-formaldehyde polymers led to the formation of sulfur groups on the surface of magnetic NPs, promoting the binding of heavy metal ions to the nanoparticles. The adsorption behavior of the synthesized adsorbent for various heavy metal ions was investigated. The results showed that synthesized nanosorbent have the ability to eliminate and extract chromium (II) and cobalt (II) from aqueous solutions. It is evident from the obtained results that the Langmuir equation fitted well the experimental data of both metal ion adsorption with a higher correlation

coefficient compared with the Freundlich equation. Thus, a single-layer adsorption mechanism by an adsorbent with a homogeneous surface can be deduced.

Acknowledgments

We are grateful to Islamic Azad University for its financial support.

Disclosure statement

No potential conflict of interest was reported by the authors.

ORCID

Somayyeh R. Mansour : 0000-0003-2487-0978

References

[1] A. Özcan, A.S. Özcan, *J. Hazard. Mater.*, **2005**, *125*, 252–259. [CrossRef], [Google Scholar], [Publisher]

[2] A. Kara, L. Uzun, N. Besirli, A. Denizli, *J. Hazard. Mater.*, **2004**, *106*, 93–99. [CrossRef], [Google Scholar], [Publisher]

[3] H.S. Altundogan, S. Altundogan, F. Tümen, M. Bildik, *Waste Manage.*, **2002,** *22*, 357–363 [CrossRef], [Google Scholar], [Publisher]

[4] D. Mishra, K.K. Senapati, C. Borgohain, A. Perumal, *J. Nanotechnol.*, **2012**, *6*, 323145. [CrossRef], [Google Scholar], [Publisher]

[5] G. Giani, S. Fedi, R. Barbucci, *Polymers.*, **2012,** *4*, 1157–1169.[CrossRef], [Google Scholar], [Publisher]

[6] T.K. Nguyen, B. Thanha, A.W. Luke, *Nano Today*, **2010**, *5*, 213–230. [CrossRef], [Google Scholar], [Publisher]

[7] I. Šafařík, K. Horská, M. Šafaříková, *Magnetic Nanoparticles for Biomedicine,* Springer: Dordrecht, **2011**, pp. 363–372. [CrossRef], [Google Scholar], [Publisher]

[8] S. Babel, T.A. Kurniawan, *J. Hazard. Mater.,* **2003,** *97*, 219–243. [CrossRef], [Google Scholar], [Publisher]

[9] Y. Li, G. Dong, J. Li, J. Xiang, J. Yuan, H. Wang, X. Wang, *Ecotoxicol. Environ. Saf.,* **2021**, *219*, 112319. [CrossRef], [Google Scholar], [Publisher]

[10] M. Gao, L. Deng, X. Kang, Q. Fu1, K. Zhang, M. Wang, Zh. Xia, D. Gao1, *J. Chromatogr. A*, **2020**, *1629*, 461476. [CrossRef], [Google Scholar], [Publisher]

[11] L. You, K. Xu, G. Ding, X. Shi, J. Li, Sh. Wang, J. Wang, *J. Mol. Liq.,* **2020**, *320*, 114456. [CrossRef], [Google Scholar], [Publisher]

[12] U. Chen, M. Zhana, F. Fu, J. Li, Z. Lin, *J. Chromatogr. A*, **2018**, *1567*, 136–146. [CrossRef], [Google Scholar], [Publisher]

[13] K. Hu, Y. Shia, W. Zhuc, J. Caie, W.Zhaob, , H. Zenga , Zh.Zhanga, Sh. Zhangd, *Food Chem.,* **2021,** *339*, 128079. [CrossRef], [Google Scholar], [Publisher]

[14] K.Z. Elwakeel, M. Rekaby, *J. hazard. Mater.,* **2011**, *188*, 10–18. [CrossRef], [Google Scholar], [Publisher]

[15] B. Al-Rashdi, C. Tizaoui, N. Hilal, *Chem. Eng. J.*, **2010**, *183*, 294–302. [CrossRef], [Google Scholar], [Publisher]

[16] A. Wasif Shaikh, S. Deokar, K. Mulani, N. Chavan, C. Raman Rajan, S. Ponrathnam, *Adv. J. Chem. A*, **2020**, *3*, 36–48. [CrossRef], [Google Scholar], [Publisher]

[17] R. Junejo, Sh. Memon, F. Durmaz, A.A. Memon, F. Nisa Memon, N.Sh. Jalbani, S.S. Memon, A.A. Bhatti, *Adv. J. Chem. A*, **2020**, *3*, S680–S691. [CrossRef], [Google Scholar], [Publisher]

[18] A. Dehno Khalaji, P. Machek, M. Jarosova, *Adv. J. Chem. A*, **2021**, *4*, 317–326. [CrossRef], [Publisher]

[19] M. Vahidpour, M. Moallem, J. East, K. Sarabandi, *Proc. SPIE*, **2012**, *8373*, 83731N. [CrossRef], [Google Scholar], [Publisher]

[20] A.D. Khalaji, S. Mousavi, Z. Palang Sangdevini, M. Jarosova, P. Machek, M. Dusek,

J. Sci. Islam. Repub. Iran, **2021**, *32*, 213–219. [CrossRef], [Google Scholar], [Publisher]

[21] F. Liu, K. Zhou, Q. Chen, A. Wang, W. Chen, *Adsorption Science and Technology.*, **2018,** *36*, 1456–1469. [CrossRef], [Google Scholar], [Publisher]

[22] T. Altun, H. Ecevit, *Environ. Eng. Res.*, **2020,** *25*, 426–438. [CrossRef], [Google Scholar], [Publisher]

HOW TO CITE THIS ARTICLE

P. Nejati, S. Rostamzadeh Mansour*, N. Sohrabi-Gilani. Synthesis and Characterization of a Nanomagnetic Adsorbent Modified with Thiol for Magnetic and Its Adsorption Behavior for Effective Elimination of Heavy Metal Ions . *Adv. J. Chem. A.*, **2022,** 5(1), 31-44.

DOI: 10.22034/AJCA.2021.308695.1283
URL: http://www.ajchem-a.com/article_140454.html